Investigation of Zirconium Oxide Films in Different Dissolved Hydrogen Concentration

Taeho Kim[a], Kyoung Joon Choi[a], Seung Chang Yoo[a], and Ji Hyun Kim[a,*]

[a] *School of Mechanical and Nuclear Engineering Ulsan National Institute of Science and Technology (UNIST), Ulju-gun, Ulsan 44919, Republic of Korea*
[*] *Corresponding author: kimjh@unist.ac.kr*

1. Introduction

Zirconium and its alloy have low thermal neutron capture cross section and excellent mechanical properties; therefore, they are used as nuclear fuel cladding materials in nuclear power plants. The phase of zirconium oxide contributes to mechanical properties and corrosion behaviors of zirconium oxide. To assure the safety of nuclear power plants, therefore, the oxidation characteristic and phase of zirconium oxide should be comprehensively understood.

Investigation based diffraction studies has shown that due to the compressive stresses, tetragonal phase fraction is the highest near the oxide/metal interface, where the compressive stress is relatively higher than the middle of the zirconium oxide. As oxidation time increases, the proportion of monoclinic zirconium oxide increases while that of tetragonal zirconium oxide decreases [1–3].

It has been reported that in pre-transition zirconium oxide, the volume fraction of tetragonal zirconium oxide increased near the oxide/metal (O/M) interface, and the sub-stoichiometric zirconium oxide layer was observed. The diffusion of oxygen ion through the oxide layer is the rate-limiting process during the pre-transition oxidation process, and this diffusion mainly occurs in the grain boundaries[5]. The two layered oxide structure is formed in pre-transition oxide for the zirconium alloy in high-temperature water environment. It is known that the corrosion rate is related to the volume fraction of zirconium oxide and the pores in the oxides [6]; therefore, the aim of this paper is to investigate the oxidation behavior in the pre-transition zirconium oxide in high-temperature water chemistry.

In this work, Raman spectroscopy was used for in situ investigations for characterizing the phase of zirconium oxide. In situ Raman spectroscopy is a well-suited technique for investigating in detail the characteristics of oxide films in a high-temperature corrosion environment. In previous studies [7,8], an in situ Raman system was developed for investigating the oxides on nickel-based alloys and low alloy steels in high-temperature water environment.

In this study, a specific zirconium alloy was oxidized and investigated with in situ Raman spectroscopy for 100 d oxidation with different dissolved hydrogen concentration, which is close to the first transition time of the zirconium alloy oxidation. The ex situ investigation methods such as transmission electron microscopy (TEM) was used to further characterize the zirconium oxide structure.

2. Experimental

2.1 Materials and specimen preparation

A plate of the zirconium alloy, provided by KEPCO Nuclear Fuel Co., Ltd., was used for the oxidation experiment in the primary water chemistry of pressurized water reactor. The chemical composition of the zirconium alloy is presented in Table. I.

Table. I Chemical composition of zirconium alloy

Element	Nb	Sn	Fe	O	N	C	Zr
Composition (wt. %)	0.96	0.76	0.18	0.62	0.03	0.1	Bal.

The specimens were polished before oxidation. Grits 400 to 800 SiC papers were used to polish the specimen. Next, diamond pastes of up to 1 μm and colloidal SiO_2 were used for minimizing the mechanical transformation of specimens.

2.2 Experimental system

For simulating the primary water chemistry of a pressurized water reactor, a loop and an autoclave for high temperature and pressure conditions were used. The detailed explanation about the system is illustrated in the authors' previous study [9].

Using this system, the conditions of the simulated primary water environment were set as follows: temperature of 360 ºC, pressure of 19 MPa, dissolved oxygen concentration of below 5 ppb, and boric acid and lithium hydroxide concentrations of 1200 ppm and 2 ppm, respectively. Also, the dissolved hydrogen concentration is controlled as 30 cm^3/kg for normal condition and 50 cm^3/kg for high dissolved hydrogen concentration. These water chemistry conditions were maintained during the oxidation process, for a total of 100 d.

The Raman spectroscopy measurements were made using a RamanRXN^{TM}, manufactured by Kaiser optical systems Inc., which used a 532 nm wavelength krypton ion laser with a maximum power of 100 mW. The irradiation area in the specimen of the Raman system was 100 μm^2 and the power density at the specimen was less than 10 mW/cm^2 to prevent the damage on the specimen. The in situ Raman system consists of four parts, and these include the immersion optics for moving the laser toward the sample, a notch filter for signal processing, a

band-pass filter, and a charge-coupled device detector. A detailed explanation about Raman system is shown in earlier studies [7,8]. The optical probe for in situ Raman was installed in the autoclave within a distance under 1 mm, which is lower than the maximum focal length of laser beam.

3. Results and Discussion

3.1. In situ Raman spectroscopy of zirconium alloy in simulated PWR primary water

Fig.1 shows the in situ Raman spectra of the zirconium alloy specimen oxidized for 100 d while the DH concentration was maintained at 30 cm^3/kg. The baseline correction method was applied to remove the baseline drift caused by fluorescence. From this method, it is possible to obtain the better Raman spectrum. The strong intensity peaks, originating from sapphire window and boric acid, are marked in the spectrum.

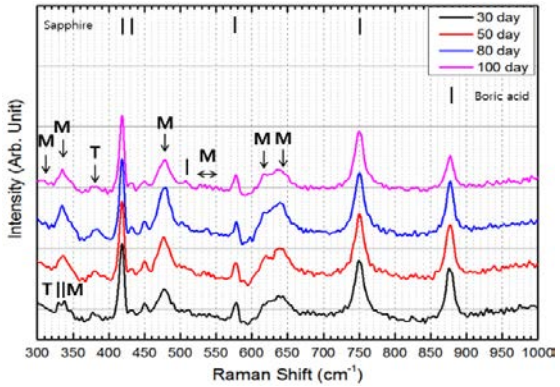

Fig.1 In situ Raman spectra of oxidized zirconium alloy specimen at four different oxidation times in primary water containing 30 cm^3/kg of dissolved hydrogen concentration

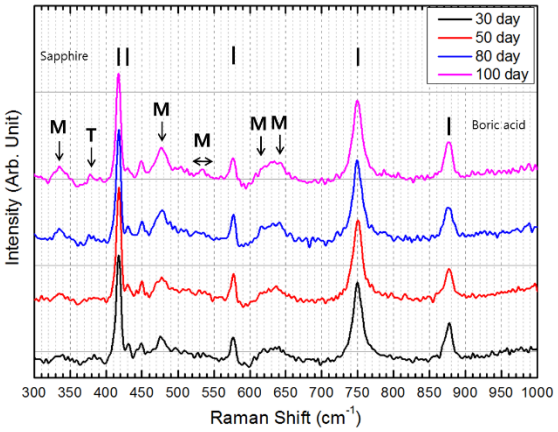

Fig. 2 In situ Raman spectra of oxidized zirconium alloy specimen at four different oxidation times in primary water containing 50 cm^3/kg of dissolved hydrogen concentration

The Raman peaks at 414, 430, 575, and 747 cm^{-1} could be attributed to sapphire window and these are produced by the tip of the Raman laser optical probe. Also, the peak observed in the range of 860 – 870 cm^{-1} corresponds to the boric acid which is dissolved in the simulated primary water [8,10,11]. The line in black is the Raman spectrum of the zirconium alloy specimen oxidized after 30 d, and the lines in blue, red, and purple are the spectra after 50, 80, and 100 d, respectively.

After 30 d oxidation, the tetragonal zirconium oxide peaks are about 330 and 380 cm^{-1}. When the oxidation time increases to 50 d, the tetragonal zirconium oxide peak at 330 cm^{-1} is merged with the monoclinic zirconium oxide. Also, the tetragonal zirconium oxide peak which is positioned about 380 cm^{-1} became weak. The monoclinic zirconium oxide peak about 620 – 640 cm^{-1} is shown in 30 d; however, it is not distinct, compared to 50, 80, and 100 d Raman spectra. As oxidation time increases, Raman peaks of monoclinic zirconium oxide become obvious, and this stands for the development of monoclinic zirconium oxide phase.

In 50 cm^3/kg DH concentration results, the tetragonal zirconium peak disappear near the 330 cm^{-1} region. Also, the intensity of tetragonal peak at 380 cm^{-1} decreased when DH is 50 cm^3/kg. This shows the dissolved hydrogen concentration influences on the phase of zirconium oxide in high temperature water environment.

3.2 Oxide Film Characterization Formed on the Zirconium Alloy

In this study, the oxide films on zirconium alloy specimens were investigated by high-resolution TEM. The zirconium alloys were oxidized for 30, 50, 80 and 100 d with different DH concentration. The results were as follows. Figure 3 shows the TEM and FFT images of oxidized zirconium alloy cross section after 30 d oxidation, and Figure 4 shows the TEM images after 50, 80 d at 30 cm^3/kg dissolved hydrogen concentration.

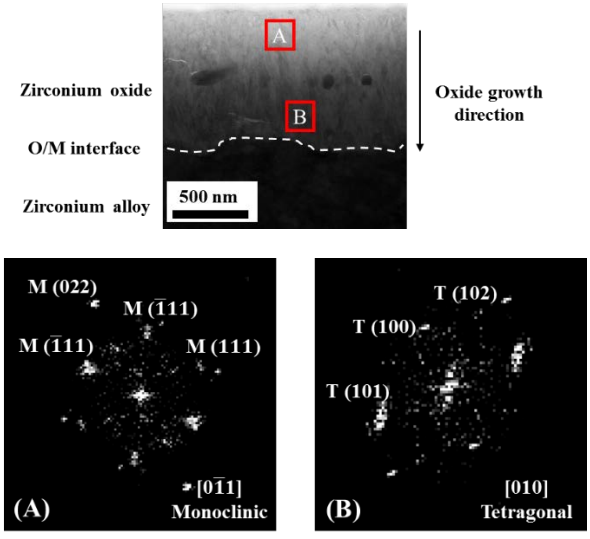

Fig. 3 TEM and FFT analysis results of oxidized zirconium alloy after 30 d oxidation.

For investigating the phase of zirconium oxide with different oxidation time, the TEM analysis was conducted. After 30 d oxidation, the oxide thickness

increased to 0.88 μm. For investigating the phase of zirconium oxide at specific position, the Fast Fourier transform (FFT) analysis was conducted from positions "A" and "B" which are marked with a red box in Fig. 3. The middle oxide which can be represented as A is analyzed as monoclinic, and the O/M interface, which can be represented as "B" is analyzed as tetragonal zirconium oxide phase. It is well-matched with in situ Raman spectroscopy results. The oxide thickness is below 1 μm; therefore, the tetragonal zirconium oxide peak can be shown in Raman spectrum after 30 d.

Fig. 4 is the TEM image of oxidized zirconium alloy after 50 and 80 d, respectively. The oxide thickness is increased from 1.46 μm to 2.27 μm as oxidation time increases from 50 d to 80 d.

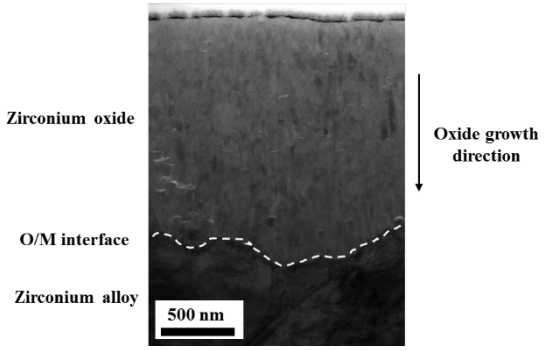

(a) 50 d

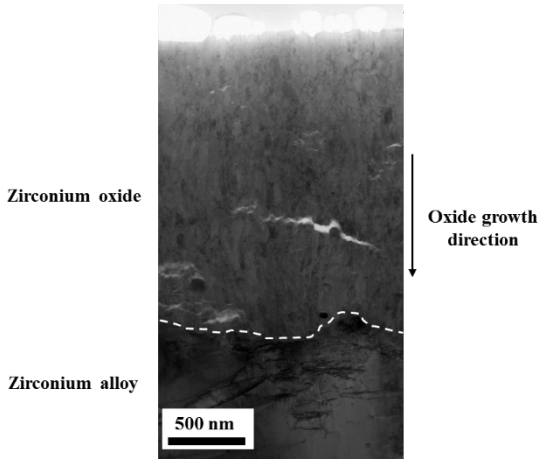

(b) 80 d

Fig. 4 TEM analysis results of oxidized zirconium alloy after (a) 50 and (b) 80 d oxidation at 30 cm^3/kg DH concentration

Fig. 5 is the TEM image of oxidized zirconium alloy after 100 d. The oxide thickness is increased to 2.44 μm as oxidation time increases to 100 d. The d-spacing of positions "A", "B", and "C" are explained, and the zirconium oxide phases located at these three sites are determined using JCPDS diffraction reference data (37-1484, 42-114, 50-1087; zirconium oxide). The FFT analysis results show that the oxide phase of positions "A" and "B" are monoclinic zirconium oxide, especially (110) and (120) planes. This means that the top and middle regions of zirconium oxide are monoclinic dominant zirconium oxide. The tetragonal zirconium oxide, which has (102) and (211) planes, is shown in position "C," which represents the O/M interface. It shows that the tetragonal zirconium oxide is always positioned near the O/M interface during the zirconium oxidation process.

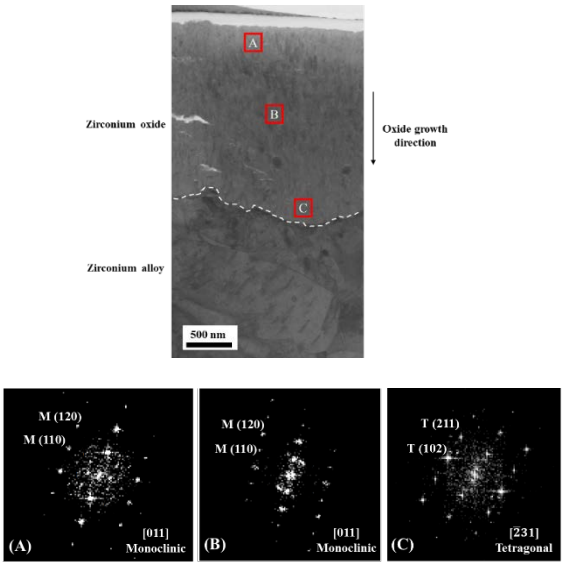

Fig. 5 TEM and FFT analysis results of oxidized zirconium alloy after 100 d oxidation.

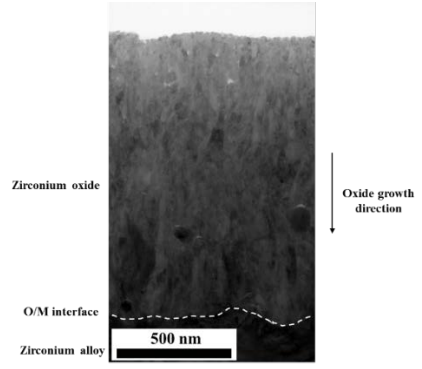

(a) 30 d

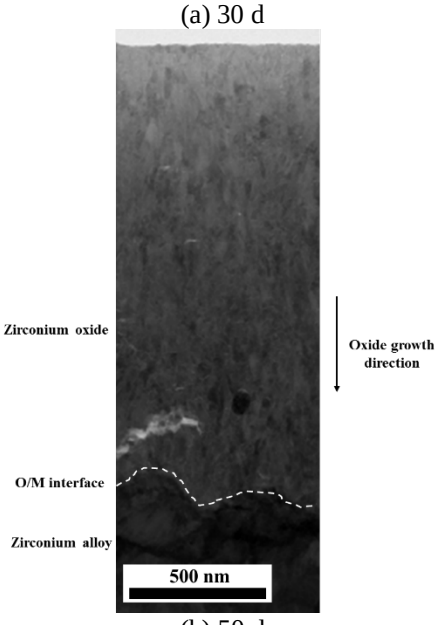

(b) 50 d

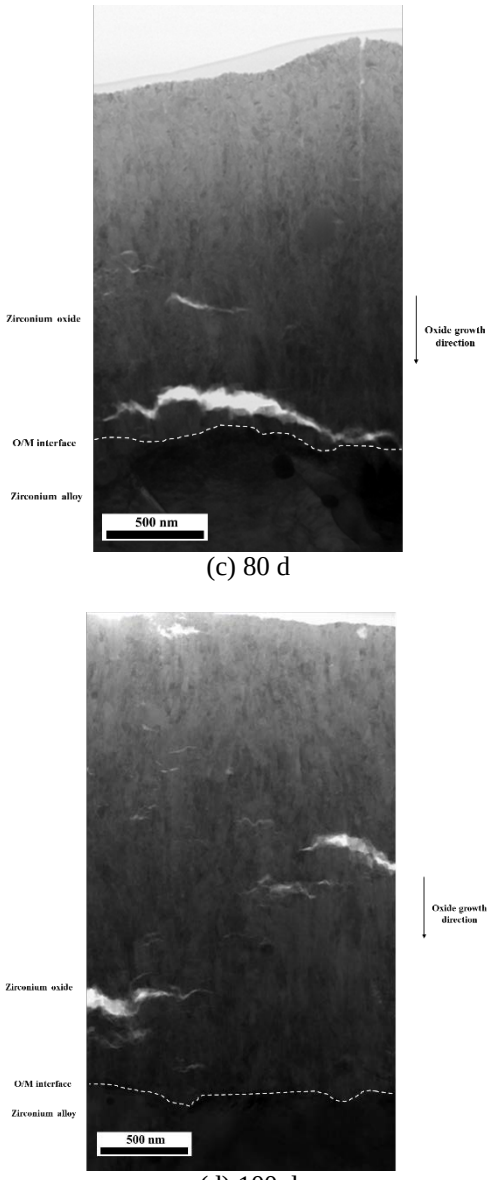

Fig. 6 TEM images of oxidized zirconium alloy during 100 d oxidation at 50 cm^3/kg DH concentration

Fig. 6 shows the TEM analysis results of oxidized zirconium alloy at 50 cm^3/kg DH concentration with different oxidation time. The further analysis will be conducted for investigating the phase of zirconium oxide.

4. Conclusions

In this study, in situ Raman and TEM analysis were conducted for investigating the phase transformation of zirconium alloy in primary water. From this study, the following conclusions are drawn:

1. The zirconium alloy was oxidized in primary water chemistry for 100 d, and Raman and TEM were measured after 30, 50, 80, and 100 d from start-up.

2. TEM and FFT analysis showed that the zirconium oxide mostly consisted of the monoclinic phase. The tetragonal zirconium oxide was just found near the O/M interface.

ACKNOWLEDGMENT

This work was financially supported by the International Collaborative Energy Technology R&D Program (No. 20138530030010 and 20168540000030) of the Korea Institute of Energy Technology Evaluation and Planning (KETEP) which is funded by the Ministry of Trade Industry and Energy.

REFERENCES

[1] P. Frankel, J. Wei, E. Francis, A. Forsey, N. Ni, S. Lozano-Perez, The effect of Sn on corrosion mechanisms in advanced Zr-cladding for pressurised water reactors, Zircon. Nucl. Ind. 17th. 61 pp. 4200–4214, 2013

[2] A. Garner, A. Gholinia, P. Frankel, M. Gass, I. MacLaren, M. Preuss, The microstructure and microtexture of zirconium oxide films stiudied by transmission electron backscatter diffraction and automated crystal orientation mapping with transmission electron microscopy, Acta Mater. 80 pp. 159–171, 2014

[3] W. Qin, C. Nam, H.L. Li, J. A, Szpunar, Tetragonal phase stability in ZrO2 film formed on zirconium alloys and its effects on corrosion resistance, Acta Mater. 55 pp. 1695–1701, 2007

[4] A. Kikas, J. Aarik, V. Kisand, K. Kooser, T. Käämbre, H. Mändar, Effect of phase composition on X-ray absorption spectra of ZrO_2 thin films, J. Electron Spectros. Relat. Phenomena. 156158, pp. 303–306, 2006

[5] R.J. Nicholls, N. Ni, S. Lozano-Perez, A. London, D.W. McComb, P.D. Nellist, Crystal structure of the ZrO phase at zirconium/zirconium oxide interfaces, Adv. Eng. Mater. 17 pp. 211–215, 2015

[6] N. Ni, S. Lozano-Perez, J. Sykes, C. Grovenor, Quantitative EELS analysis of zirconium alloy metal/oxide interfaces, Ultramicroscopy. 111, pp. 123–130, 2010

[7] N. Ni, D. Hudson, J. Wei, P. Wang, S. Lozano-Perez, G.D.W. Smith How the crystallography and nanoscale chemistry of the metal/oxide interface develops during the aqueous oxidation of zirconium cladding alloys, Acta Mater. 60, pp. 7132–7149, 2012

[8] T. Kim, J. Kim, K.J. Choi, S.C. Yoo, S. Kim, J.H. Kim, Phase Transformation of Oxide Film in Zirconium Alloy in High Temperature Hydrogenated Water, Corros. Sci. 99, 134–144, 2015

[9] Y. Lei, Y. Ito, N.D. Browning, T.J. Mazanec, Segregation Effects at Grain Boundaries in Fluorite-Structured Ceramics, J. Am. Ceram. Soc. 85, pp. 2359–2363, 2002

[10] J. Hu, A. Garner, N. Ni, A. Gholinia, R.J. Nicholls, S. Lozano-Perez, et al., Identifying suboxide grains at the metal-oxide interface of a corroded Zr-1.0%Nb alloy using (S)TEM, transmission-EBSD and EELS, Micron. 69, pp. 35–42, 2015

[11] L. Kurpaska, I. Jozwik, J. Jagielski, Study of sub-oxide phases at the metal-oxide interface in oxidized pure zirconium and Zr-1.0% Nb alloy by using SEM/FIB/EBSD and EDS techniques, J. Nucl. Mater. 476, pp. 56-62, 2016